Computers in Biology and Medicine 109 (2019) 112–120

Contents lists available at ScienceDirect

Computers in Biology and Medicine

journal homepage: www.elsevier.com/locate/compbiomed

Dynamically NAND gate system on DNA origami template

Zhen Tang[a], Zhi-Xiang Yin[a,*], Xia Sun[a], Jian-Zhong Cui[b], Jing Yang[a], Ri-sheng Wang[a]

[a] School of Mathematics and Big Data, AnHui University of Science&Technology, Huainan, 232001, AnHui, China
[b] School of Electronic and Information Engineering, AnHui University of Science&Technology, Huainan, 232001, AnHui, China

ARTICLE INFO

Keywords:
DNA origami
Hybridization chain reaction
NAND gate
DNA computing
Molecular logic gate

ABSTRACT

Molecular logic gates play an important role in many fields and DNA-based logic gates are the basis of DNA computers. A dynamically NAND gate system on the DNA origami template is established in this paper. Naturally, the system is stable in solution without any reaction. Different logical values are mapped into different DNA input strands. When logical values are entered into the system, the corresponding DNA input strands undergo a directed hybridization chain reaction (HCR) at corresponding positions on the DNA origami template. The operation results are identified by disassembly between the nanogold particles (AuNPs) and DNA origami template. The nanogold particles remain on the DNA origami template, indicating that the result is true; The nanogold particles are dynamically separated from the DNA origami template, indicating that the result is false. The simulation of the system through Visual DSD shows that the reaction strictly followed the designed direction, and no error products are generated during the reaction. These simulation results show that the system has the advantages of feasibility, stability and intelligence.

1. Introduction

Since Adleman solved the Hamiltonian path problem of directed graphs with DNA coding for the first time [1], DNA computing has attracted the attention of many scholars. In recent years, the researches of DNA computing have been fruitful. We have reasons to believe that DNA computers will lead us to a new era of computing in the near future. In 2004, Dirks proposed the hybridization chain reaction (HCR), which used DNA hybridization to expand DNA strands for signal amplification [2]. In the reaction, two kinds of hairpin-shaped DNA oligonucleotides coexist stably without a kind of linear DNA oligonucleotide, called the initiator. When the initiator is poured into the test tube containing two hairpins, the hybridization chain reaction is induced. The hairpins are opened alternately, and hybridize with one another to form a nicked double-stranded DNA polymer. The hybridization chain reaction is widely used in combinatorial optimization, analytical chemistry, biosensors and medical signal detection [3–5]. In 2006, DNA origami was first proposed by Rothemund [6]. In the same year, Qian and coworkers established an asymmetric simulated Chinese map by using DNA origami [7]. The successful construction of this map demonstrated the ability of DNA origami to construct asymmetric patterns. Compared with traditional self-assembly methods, DNA origami can self-assemble precisely more complex structures on nanometer scale [8,9]. These advantages enable DNA origami to be utilized as a basic template for assembling functional AuNPs, carbon nanotubes and proteins into sophisticated structures. In 2010, Gu designed a 'three-handed, four-legged' DNA walker based on DNA origami. The 'foot' can rotate clockwisely by 120° on the DNA origami template. The 'hand' can receive AuNPs modified on the DNA origami template during the rotational walking. The construction of this DNA walker provided ideas for the design of medical carriers [10]. In 2012, Pei and coworkers completed the logic operation by reconfiguring the tetrahedral DNA nanostructures [11]. In 2013, biped DNA walkers took a critical step in DNA origami orbits [12]. In 2014, DNA origami robots were used for routine computing [13]. In the same year, Wang proposed molecular logic gates on the DNA origami nanostructures for microRNA diagnostics [14]. Koirala and coworkers built mechanochemical sensors based on DNA origami nanostructures [15]. In 2016, Yang and coworkers developed a strategy based on DNA strand displacement to control the release of AuNPs on the DNA origami template [16]. Yang solved the operation problems of OR gate, AND gate and three-input majority gate based on this strategy. Experimental results showed that this strategy proposed was feasible. Zhang and coworkers used a series of DNAzyme-based logic gates to control DNA tile self-assembly onto a prescribed DNA origami frame [17]. Tikhomirov and coworkers proposed a method of fractal assembly of micron-scale DNA origami arrays with arbitrary patterns [18]. In that paper, a square DNA origami tile with a pattern on the surface was used as a basic building unit, and

* Corresponding author.
E-mail address: zxyin66@163.com (Z.-X. Yin).

https://doi.org/10.1016/j.compbiomed.2019.04.026
Received 16 April 2019; Received in revised form 21 April 2019; Accepted 21 April 2019

patterns such as Mona Lisa and rooster were constructed. The construction and successful implementation of this assembly method illustrated the advantages of DNA origami spatial addressability. In 2019, Chao and coworkers used the single-molecule DNA navigator to solve the maze problem on a DNA origami template. This single-molecule navigator can search all the paths of the maze, and finally only the correct paths were preserved [19]. Tang constructed and optimized the aptamer-enabled DNA boxes [20]. In addition, Wang and coworkers built the intelligent molecular logic circuits based on well-designed H-shaped DNA nanostructures [21]. Recently, DNA origami nanostructures have also been widely used in the fields of bioanalysis and drug delivery. Zhang constructed a poly-aptamer-drug system for drug delivery [22]. Ouyang constructed the drug delivery nanocarriers [23]. The nanocarriers were assembled based on the rolling ring amplification (RCA). In 2019, Rozita selectively reviewed the recent advances in DNA-based biosensors. These biosensors were used to detect cancer microRNA, toxic metal ion and infectious microbes based on various signal amplification strategies [24]. The DNA nanostructure is a good drug carrier and has unique advantages in cancer therapy. In 2017, Wu described these different types of DNA nanostructure-based drug delivery nanosystems and introduced the advantages of these systems in medical applications [25]. In 2018, Mason described the principles of common DNA walkers and the applications of DNA walkers in bioanalysis [26].

In this paper, we construct a dynamically NAND gate system based on the hybridization chain reaction to solve the NAND gate operation problem. HCR and DNA origami structures have proven to be very suitable for this type of application [27–34]. The system consists of two parts: a constructed origami template and four kinds of auxiliary strands. The sequence layout of the DNA strands in the system are carefully designed to ensure that the system is stable in solution without any reaction.

During the operation, the input values of the NAND gate are mapped into DNA strands of different sequence layout. Once there is a value input, the corresponding DNA strand enters the system, and it performs a hybridization chain reaction on a specific path. Finally, The operation results are identified by disassembly between the AuNPs and DNA origami template. If two AuNPs remain on the DNA origami template, then the result is true. If two AuNPs are dynamically separated from the DNA origami template, then the result is false. The simulation of the dynamically NAND gate system by Visual DSD (a design and analysis tool for DNA strand displacement systems) proves that the system has good feasibility, stability and intelligence.

2. NAND gate and hybridization chain reaction

2.1. NAND gate

Logic gates play an important role in various fields. For example, molecular logic gates are the basis of DNA computers, and intracellular molecular logic gates have a great significance for medical treatment. An ideal DNA logic gate system for medical purposes would have high cell permeability. Common logic gates include OR gates, AND gates, NOT gates, NAND gates and NOR gates.

The NAND gate refers to the superposition of the AND gate and the NOT gate. The AND gate operation is performed first and then the NOT gate is performed. See 2.1 for the NAND gate logic expression and Table 1 for the truth table.

$$F = (A \cdot B)' = (A') + (B') \tag{2.1}$$

The NAND gate only has a false result when the input values are all true, otherwise, the result is true.

2.2. Hybridization chain reaction

In 2004, Dirks first proposed the HCR [2]. The principle of HCR is to induce hybridization of two different types of DNA molecules with hairpin structure by using an initial strand and alternately opening the hairpin structure to form a double-stranded DNA polymer with a nick. The formation of the DNA polymer can be carried out at room temperature without the temperature changes and enzymes. The reaction principle is shown in Fig. 1. The two DNA strands T_1 and T_2 coexist stably in solution without any hybridization reaction. T_1 DNA strands have a common sequence layout of the structure 5′-toehold-stem-loop-stem*-3′($5' - a - b - c - b* - 3'$); correspondingly, the T_2 DNA strands, freely diffusing in solution, have a common sequence layout of the structure 5′-toehold-stem-loop-stem*-3′($5' - c^* - b - a^* - b^* - 3'$), as shown in Fig. 1a. Initiator strands I have a sequence layout of $5' - b^* - a^* - 3'$. When the initiation strands I are added, the $a* - b*$ of initiation strand I is complementary to the toehold a and stem b of T_1, and the hairpin of T_1 is opened, exposing $c - b^*$ (see Fig. 1b). The exposed $c - b^*$ of DNA strand T_1 and $c^* - b$ of DNA strand T_2 are complementary by base pairing, and the hairpin of T_2 is opened, exposing $a^* - b^*$ (see Fig. 1c). The exposed $a^* - b^*$ of DNA strand T_2 continues to react with the next DNA strand T_1, opening the hairpin structure and cycling in sequence. Eventually, alternate hybridization results in a long, nicked double-stranded DNA polymer (see Fig. 1d).

Table 1
NAND truth table.

A	B	F
0	0	1
0	1	1
1	0	1
1	1	0

3. Dynamically NAND gate system on DNA origami template

3.1. The composition of the system

The dynamically NAND gate system on the DNA origami template is mainly composed of two parts: a constructed origami template and four kinds of auxiliary strands. In this system, the four kinds of auxiliary strands exist in large quantities and do not react with the stable coexistence of the constructed DNA origami template. The following describes the composition of the system.

The circular genomic DNA from the virus M13mp18 [6] is folded into a two-dimensional rectangle origami template using staples, as shown in Fig. 2a. Two rows of DNA strands arranged in a straight line are anchored on a DNA origami template, as shown in Fig. 2d. In this system, there are four entries on the DNA origami template, H_{A0ent}, H_{A1ent}, H_{B0ent} and H_{B1ent}, which correspond to four input values, $A = 0$, $A = 1$, $B = 0$, $B = 1$, respectively. When an input value enters the system, a directed hybridization chain reaction begins at the corresponding entry, with the AuNPs N1 and N2 as the cut-off points, the reaction directions are recorded as $\overrightarrow{L1_0} \rightarrow N1 \leftarrow \overleftarrow{L1_1}$ and $\overrightarrow{L2_0} \rightarrow N2 \leftarrow \overleftarrow{L2_1}$, respectively. The reaction direction of path $\overrightarrow{L1_0}$ is from left to right, arranged in the order $H_{A0ent} \rightarrow H_{L1} \rightarrow \cdots \rightarrow H_{L1} \rightarrow H_{A0end}$. H_{A0ent} is called the entrance strand and has a sequence layout of the structure 5′-h_{ori}-toehold-stem-loop-stem*-3′ ($5' - h_{ori} - A0 - b_1 - c_1 - b_1^* - 3'$); h_{ori} and the sticky end h_{ori}^* extending from the DNA origami template are complementary by base pairing, and thus, the strand H_{A0ent} is anchored on the origami template. The strands H_{L1} are arranged in a straight line on the DNA origami template (In the original design, the strands H_{L1} in the four paths are the same; unfortunately, in the reaction, the reaction direction cannot be completely directed according to the designed straight line, and an intersection phenomenon occurs. Thus, for path $\overrightarrow{L1_0}$, $\overleftarrow{L1_1}$, the design of the strand H_{L1} is the same. For the path $\overrightarrow{L2_0}$, $\overleftarrow{L2_1}$, we design a different strand, H_{L2}; this difference can avoid the intersection in the reaction).

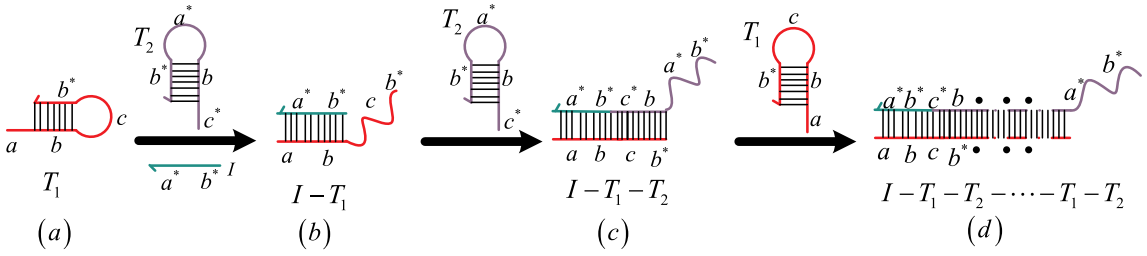

Fig. 1. Basic reaction process of HCR.

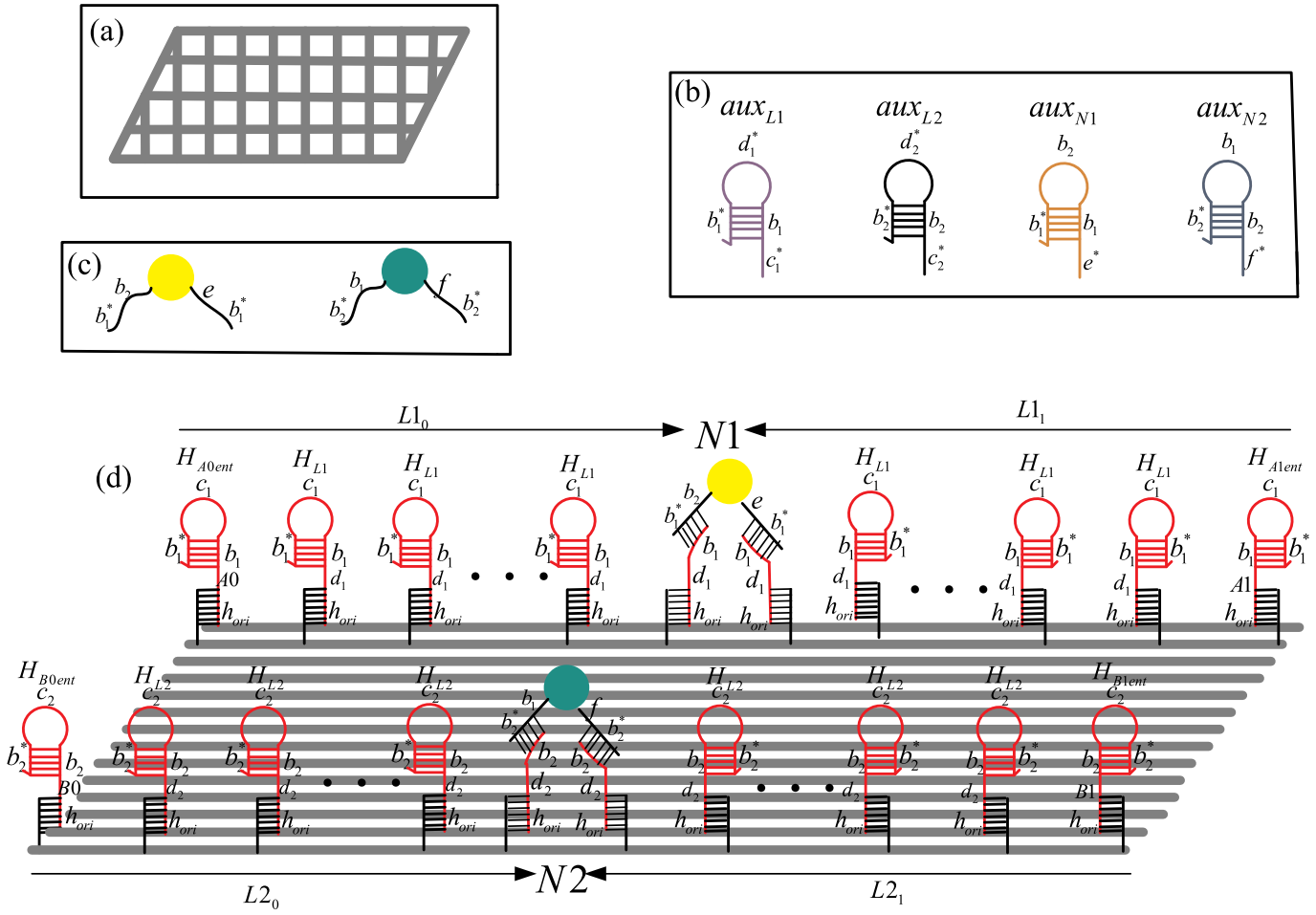

Fig. 2. (a) Rectangular DNA origami template. (b) Four kinds of auxiliary DNA strands aux_{L1}, $aux_{L2}aux_{N1}$, aux_{N2}. (c) AuNPs, N1 and N2. (d) The constructed origami template.

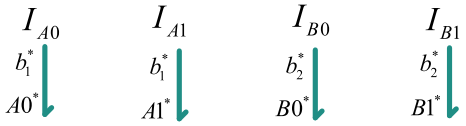

Fig. 3. The schematic diagram of I_{A0}, I_{A1}, I_{B0} and I_{B1}.

The strands H_{L1} have a common sequence layout of the structure 5′-h_{ori}-toehold-stem-loop-stem*-3′(5′ − h_{ori} − d_1 − b_1 − c_1 − b_1^* − 3′). H_{A0end} is called the end strand and has a sequence layout of 5′ − h_{ori} − d_1 − b_1 − 3′; b_1 of H_{A0end} and b_1^* of AuNP N1 (see Fig. 2c) are complementary by base pairing such that the AuNP N1 can be attached to the strand H_{A0end}. The reaction direction of path $\overleftarrow{L1_1}$ is from right to left, arranged in the order $H_{A1end} \leftarrow H_{L1} \leftarrow \cdots \leftarrow H_{L1} \leftarrow H_{A1ent}$. H_{A1ent} is called the entrance strand and has a sequence layout of 5′-h_{ori}-toehold-stem-loop-stem*-3′ (5′ − h_{ori} − $A1$ − b_1− c_1− b_1^* − 3′). H_{A1end} is called the end strand and is designed like H_{A0end}. The reaction direction of path $\overrightarrow{L2_0}$ is from left to right, arranged in the order $H_{B0ent} \rightarrow H_{L2} \rightarrow \cdots \rightarrow H_{L2} \rightarrow H_{B0end}$. H_{B0ent} is called the entrance strand and has a sequence layout of 5′-h_{ori}-toehold-stem-loop-stem*-3′(5′ − h_{ori} − $B0$ − b_2 − c_2 − b_2^* − 3′). The strands H_{L2} have a common sequence layout of 5′-h_{ori}-toehold-stem-loop-stem*-3′(5′ − h_{ori} − $A1$ − b_1− c_1− b_1^* − 3′). H_{B0end} is called the end strand and has a sequence layout of 5′ − h_{ori} − d_2 − b_2 − 3′; b_2 of H_{B0end} and b_2^* of AuNP N2 (see Fig. 2c) are complementary by base pairing such that the AuNP N2 can be attached to the strandH_{B0end}. The reaction direction of path $\overleftarrow{L2_1}$ is from right to left, arranged in the order $H_{B1end} \leftarrow H_1 \leftarrow \cdots \leftarrow H_1 \leftarrow H_{B1ent}$. H_{B1ent} is called the entrance strand and has a sequence layout of 5′-h_{ori}-toehold-stem-loop-stem*-3′ (5′ − h_{ori} − $A1$ − b_1− c_1− b_1^* − 3′). H_{B1end} is called the end strand and is designed like H_{B0end}.

In the dynamically NAND gate system, four kinds of auxiliary

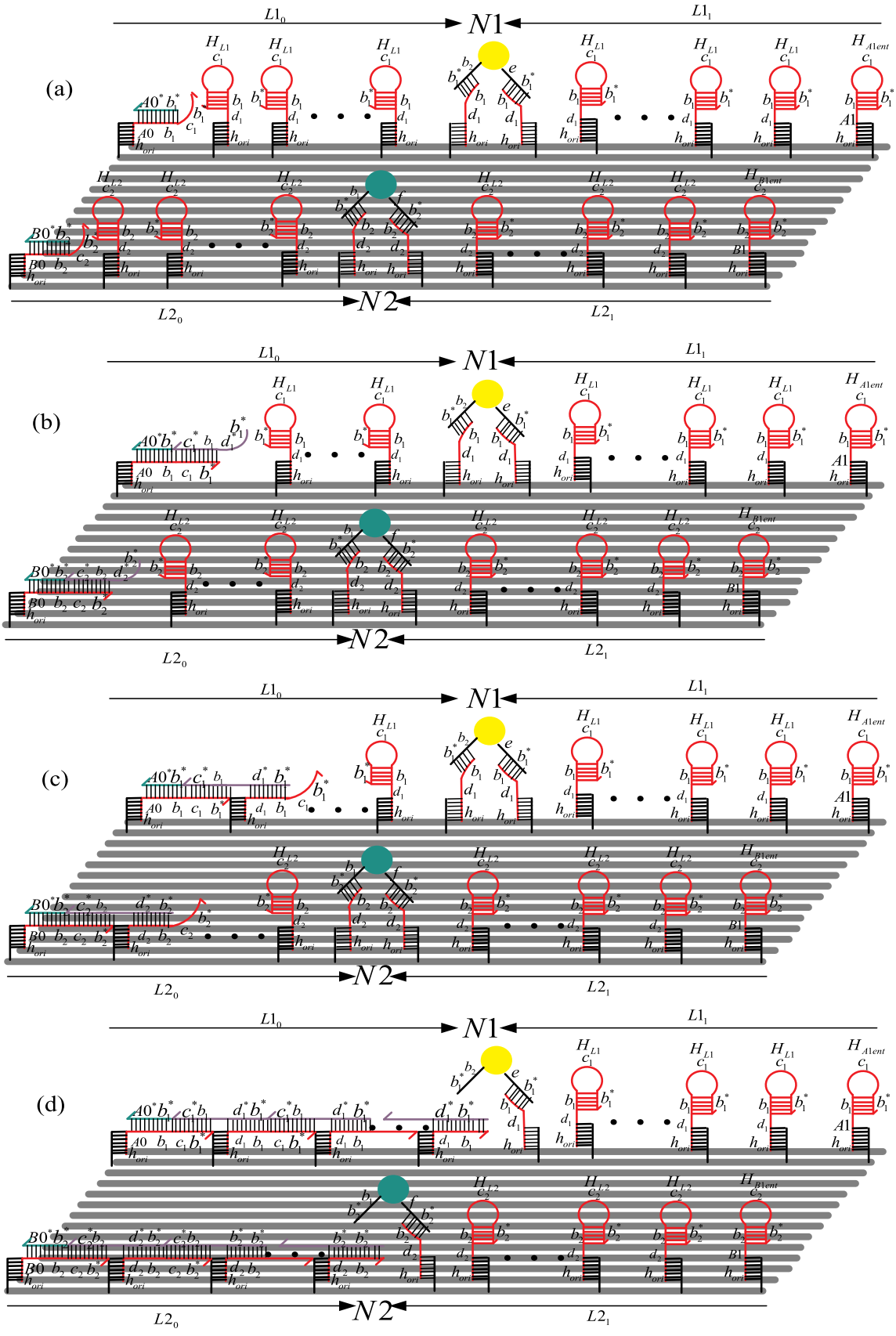

Fig. 4. (a) The schematic diagram of combining I_{A0} and H_{A0ent} and combining I_{B0} and H_{B0ent}. (b) The schematic diagram of combining H_{A0ent} and aux_{L1} and combining H_{B0ent} and aux_{L2}. (c) The schematic diagram of combining aux_{L1} and H_{L1} and combining aux_{L2} and H_{L2}. (d) The reaction is completed, and the AuNPs N1 and N2 remain on the origami template, indicating that the result is true.

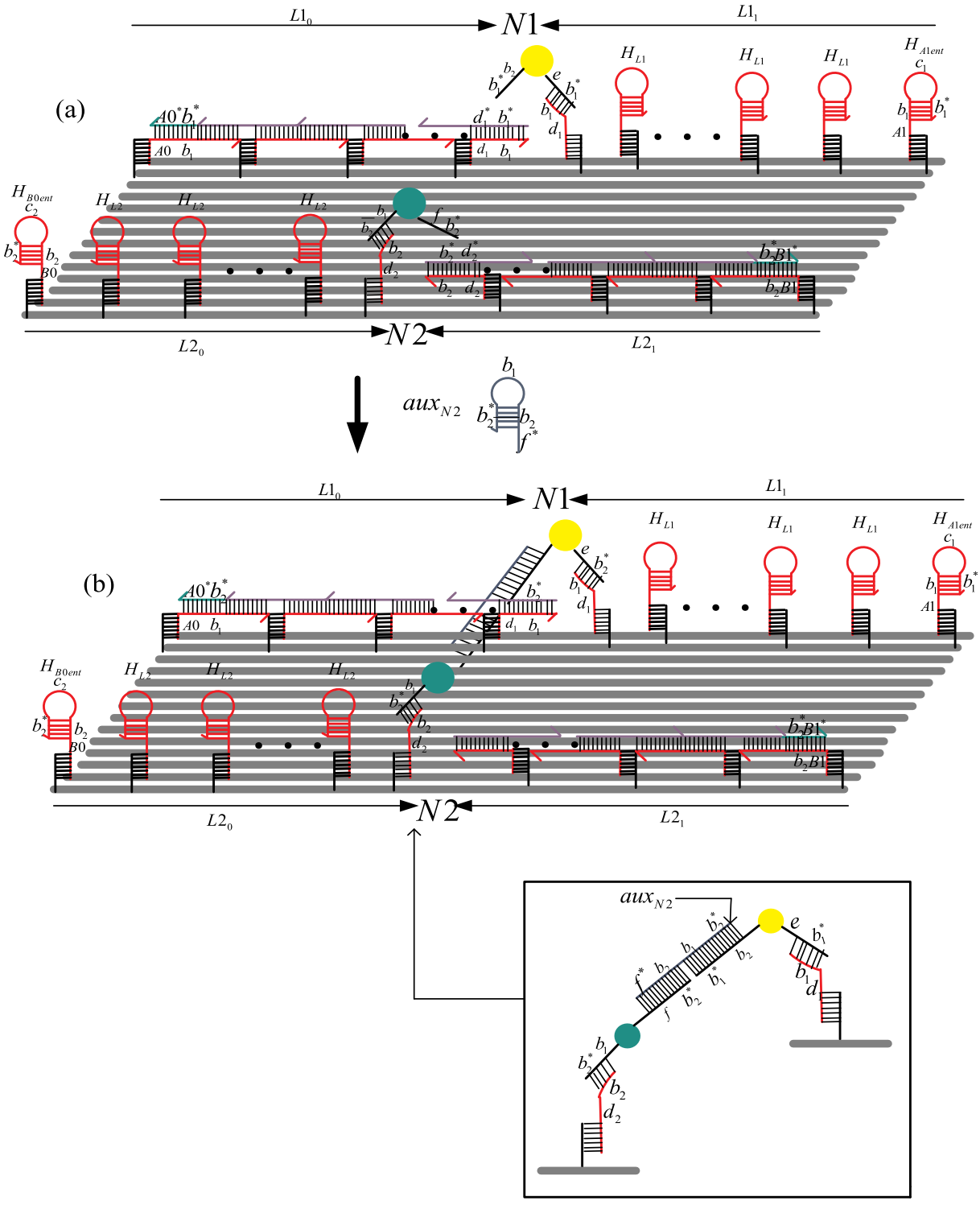

Fig. 5. (a) The left end of the AuNP N1 and the right end of the AuNP N2 are separated. (b) The reaction is completed, and the N1 and N2 remain on the origami template, indicating that the result is true.

strands are required, which are called aux_{L1}, aux_{L2}, aux_{N1} and aux_{N2}, respectively, as shown in Fig. 2b. These auxiliary strands do not need to be anchored on the DNA origami template, but they are stored in large quantities in the test tube solution. The strands aux_{L1} and aux_{L2} are used to assist the directional reaction on $\overrightarrow{L1_0}$, $\overleftarrow{L1_1}$ and $\overrightarrow{L2_0}$, $\overleftarrow{L2_1}$, respectively, while aux_{N1} and aux_{N2} are used to assist in the disassembly between the AuNPs and DNA origami template. The strands aux_{L1} have a common sequence layout of 5′-toehold-stem-loop-stem*-3′ ($5' - c_1^* - b_1 - d_1^* - b_1^* - 3'$); the strands aux_{L2} have a common sequence layout of 5′-toehold-stem-loop-stem*-3′ ($5' - c_2^* - b_2 - d_2^* - b_2^* - 3'$); the strands aux_{N1} have a common sequence layout of 5′-toehold-stem-loop-stem*-3′ ($5' - e^* - b_1 - b_2 - b_1^* - 3'$); and the strands aux_{N2} have a common sequence layout of 5′-toehold-stem-loop-stem*-3′ ($5' - f^* - b_2 - b_1 - b_2^* - 3'$).

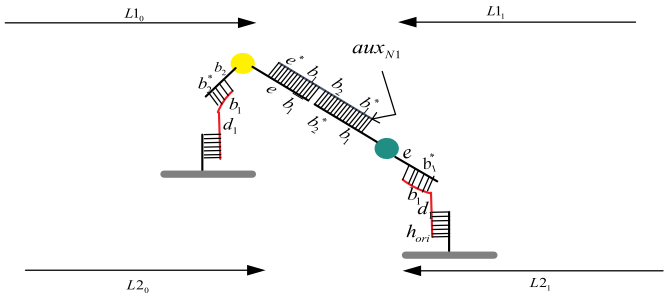

Fig. 6. The reaction is completed, and N1 and N2 remain on the origami template, indicating that the result is true.

3.2. The implementation of the NAND gate

3.2.1. The design of the input strands

Enter a representative strand of $A = 0$ called I_{A0}, with a sequence layout of $5' - b_1^* - A0^* - 3'$; enter a representative strand of $A = 1$ called I_{A1}, with a sequence layout of $5' - b_1^* - A1^* - 3'$; enter a representative strand of $B = 0$ called I_{B0}, with a sequence layout of $5' - b_2^* - B0^* - 3'$; and enter a representative strand of $B = 1$ called I_{B1}, with a sequence layout of $5' - b_2^* - B1^* - 3'$, as shown in Fig. 3.

When $A = 0$, $B = 0$ are entered, strand I_{A0} and strand I_{B0} enter the NAND gate system. HCR is performed on path $\overrightarrow{L1_0}$; $b_1^* - A0^*$ of I_{A0} and $b_1 - A0$ of H_{A0ent} are complementary by base pairing, and the hairpin structure of H_{A0ent} is opened, exposing $c_1 - b_1^*$, as shown in Fig. 4a. The exposed $c_1 - b_1^*$of H_{A0ent} and $c_1^* - b_1$ of aux_{L1} are complementary by base pairing, and the hairpin structure of aux_{L1} is opened, exposing $d_1^* - b_1^*$, as shown in Fig. 4b. The exposed $d_1^* - b_1^*$ of aux_{L1} and $d_1 - b_1$ of H_{L1} are complementary by base pairing, and the hairpin structure of H_{L1} is opened, exposing $c_1 - b_1^*$, as shown in Fig. 4c. The reaction proceeds alternately from left to right until the $d_1^* - b_1^*$ of aux_{L1} is complementary to the $d_1 - b_1$ of H_{A0end}, the DNA single strand to which the AuNP N1 and H_{A0end} are attached is replaced, and the reaction ends. At this time, the AuNP N1 is disconnected from H_{A0end} but is still connected to H_{A1end} and remains on the DNA origami template, as shown in Fig. 4d. The hybridization chain reaction is performed on path $\overrightarrow{L2_0}$. $b_2^* - B0^*$ of I_{B0} and $b_2 - B0$ of H_{B0ent} are complementary by base pairing, and the hairpin structure of H_{B0ent} is opened, exposing $c_2 - b_2^*$, as shown in Fig. 4a. The exposed $c_2 - b_2^*$ of H_{B0ent} and $c_2^* - b_2$ of aux_{L2} are complementary by base pairing, and the hairpin structure of aux_{L2} is opened, exposing $d_2^* - b_2^*$, as shown in Fig. 4b. The exposed $d_2^* - b_2^*$ of aux_{L2} and $d_2 - b_2$ of H_{L2} are complementary by base pairing, and the hairpin structure of H_{L2} is opened, exposing $c_2 - b_2^*$, as shown in Fig. 4c. The reaction proceeds alternately from left to right until the $d_2^* - b_2^*$ of aux_{L2} is complementary to the $d_2 - b_2$ of H_{B0end}, the DNA single strand to which the AuNP N2 and H_{B0end} are attached is replaced, and the reaction ends. At this time, the AuNP N2 is disconnected from H_{B0end} but is still connected to H_{B1end} and remains on the DNA origami template, as shown in Fig. 4d.

When $A = 0$, $B = 1$ are entered, strand I_{A0} and strand I_{B1} enter the NAND gate system. The hybridization chain reaction is performed on path $\overrightarrow{L1_0}$ in the same manner as described above, we will not repeat all the details here. The AuNP N1 is disconnected from H_{A0end} but is still connected to H_{A1end} and remains on the DNA origami template, as shown in Fig. 5a. The hybridization chain reaction is performed on path $\overleftarrow{L2_1}$. The $b_2^* - B1^*$ of I_{B1} and $b_2 - B1$ of H_{B1ent} are complementary by base pairing, the hairpin structure of H_{B1ent} is opened, and the hybridization chain reaction begins. The reaction proceeds alternately from right to left until the $d_2^* - b_2^*$ of aux_{L2} is complementary to the $d_2 - b_2$ of H_{B1end}, and the DNA single strand to which the AuNP N2 and H_{B1end} are attached is replaced, as shown in Fig. 5a. The difference in this case is that the reaction has not completely ended. The $f - b_2^*$ of N2 and the $f^* - b_2$ of aux_{N2} are complementary by base pairing, and the hairpin structure of aux_{N2} is opened. The $b_1 - b_2^*$ of aux_{N2} and $b_1^* - b_2$ of N1 are complementary by pairing, and AuNPs N1 and N2 are connected together by the auxiliary strand aux_{N2}, as shown in Fig. 5b. However, N1 is still connected to H_{A1end}, and N2 is still connected to H_{B0end}. N1 and N2 remain on the DNA origami template.

When $A = 1$, $B = 0$ are entered, strand I_{A1} and strand I_{B0} enter the NAND gate system. It is essentially the same as when $A = 0$, $B = 1$ are entered, so the schematic diagram of the entire reaction is not given here, but a schematic diagram of the connection of the AuNPs on the DNA origami template is given. The hybridization chain reaction is performed on path $\overleftarrow{L1_1}$, and the DNA single strand to which the AuNP N1 and H_{A1end} are attached is displaced. The hybridization chain reaction is performed on path $\overrightarrow{L2_0}$, and the DNA single strand to which the AuNP N2 and H_{B0end} are attached is displaced. AuNPs N1 and N2 are connected together by the auxiliary strand aux_{N1}, as shown in Fig. 6. However, AuNP N1 is still connected to H_{A0end}, and AuNP N2 is still connected to H_{B1end}. N1 and N2 remain on the DNA origami template.

When $A = 1$, $B = 1$ are entered, strand I_{A1} and strand I_{B1} enter the NAND gate system. The hybridization chain reaction is performed on path $\overleftarrow{L1_1}$, and the DNA single strand to which the AuNP N1 and H_{A1end} are attached is displaced, as shown in Fig. 7a. The hybridization chain reaction is performed on path $\overleftarrow{L2_1}$, and the DNA single strand to which the AuNP N2 andH_{B1end} are attached is displaced, as shown in Fig. 7a. Then, the $e - b_1^*$ of N1 and the $e^* - b_1$ of aux_{N1} are complementary by base pairing, and the hairpin structure of aux_{N1} is opened. The $b_2 - b_1^*$ of aux_{N1} and $b_2^* - b_1$ of $N2$ are complementary by base pairing, and the connection of the N2 to the strand H_{B0end} is broken, as shown in Fig. 7b. The $f - b_2^*$ of N2 and the $f^* - b_2$ of aux_{N2} are complementary by base pairing, and the hairpin structure of aux_{N2} is opened. The $b_1 - b_2^*$of aux_{N1} and $b_1^* - b_2$ of N2 are complementary by base pairing, and the connection of the N1 to the strand H_{A0end} is broken, as shown in Fig. 7b. Thus, the AuNPs N1 and N2 are separated from the DNA origami template by the auxiliary strands aux_{N1} and aux_{N2}.

4. Discussion

In this paper, we constructed a dynamically NAND gate system on the DNA origami template. The operation results are identified by disassembly between the AuNPs and DNA origami template. Fig. 8 depicts a graph of the feasibility data obtained by simulating the system using Visual DSD. Fig. 8(a), (b), (c), and (d) show the results of simulations on the paths $\overrightarrow{L1_0}$, $\overrightarrow{L2_0}$, $\overleftarrow{L1_1}$ and $\overleftarrow{L2_1}$, respectively. In Fig. 8, inputA0, inputA1, inputB0, and inputB1 represented the input strands and their concentration were set to 20 nM auxL1 and auxL2 represented the auxiliary strands and their concentration were set to 50 nM origamiL1 and origamiL2 represented the constructed DNA origami template and their concentration were set to 10 nM. The reaction time was set to 7000s. When the input strands entered the system, the concentration of the initial material (input, aux, origami) decreased, and the concentration of the intermediate product (sp4 ~ sp13) increased. After reaching the maximum peak value, the concentration of the intermediate product gradually decreased, and their concentration tended to 0 nM after the reaction was completed. The final product (sp14) concentration increased and stabilized to 9.4 nM. The simulation results show that the system is highly feasible.

In addition, the simulation results show that the entire system stably coexists in the tube without any hybridization reaction. After the input strands entered the system, the results of this simulation were consistent with the expected results of the system and no error products were generated during the reaction. These show that the system constructed in this paper has good stability. The key reason for the system to have good stability is: the DNA strands in the system have a hairpin structure, which can effectively avoid mismatches and ensures that the reaction can proceed in the direction of the design. The reaction of the whole system is based on the hybridization chain reaction. This process

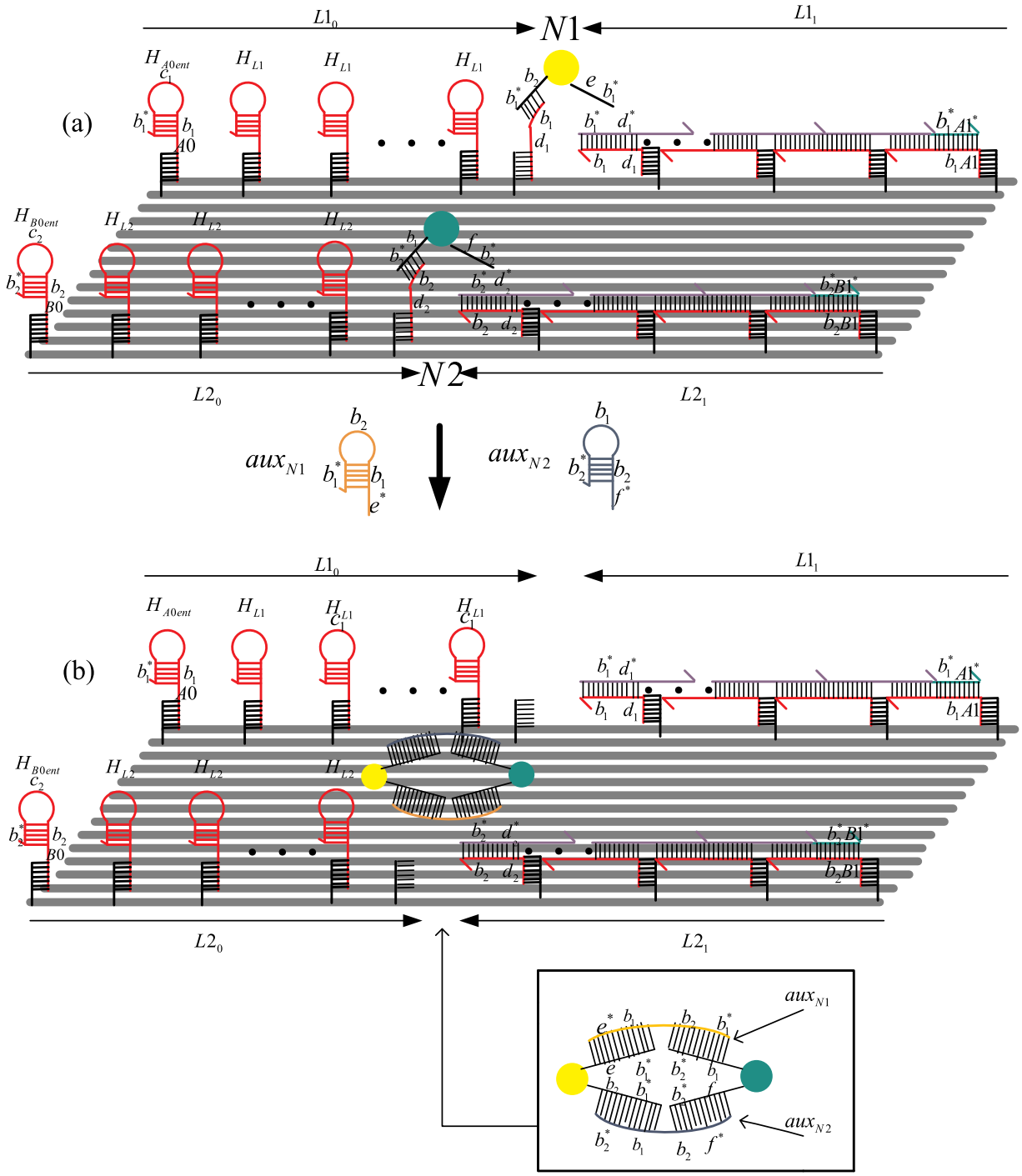

Fig. 7. (a) The right end of the AuNPs N1 and N2 are separated. (b) The reaction is completed, and the AuNPs N1 and N2 are separated from the DNA origami template, indicating that the result is false.

does not require the participation of the enzyme and proceeds spontaneously until the end of the reaction. There are some models that are too artificially involved, such as the need to manually separate and merge test tubes in the reaction. Compared with these models, the only steps involved in this paper are the addition of the input strands and the detection of the results. This shows that the system has a certain degree of intelligence.

The concentration curve of Fig. 8 contains all of the starting materials and products. Fig. 9 shows a schematic of the linkage of the final product (sp14). As seen in Fig. 9, the upper reaction proceeds in the direction of the directed path until the AuNPs are displaced and the reaction is complete.

5. Conclusion

The NAND gate is the basis of the combined logic gate, and its operation provides a better idea for constructing more complex logic gates. In this paper, we have successfully constructed a dynamic NAND gate system that can selectively and dynamically control the release of AuNPs on the DNA origami template. As the number of nanogold particles and the size of the system increase, the dynamic structural arrangements of AuNPs/origami system should solve more complex logic gate computing. Thus, the system has potential scalability. The main advantage of biocomputing solutions over traditional electronic computing solutions is that they can be directly linked to biological

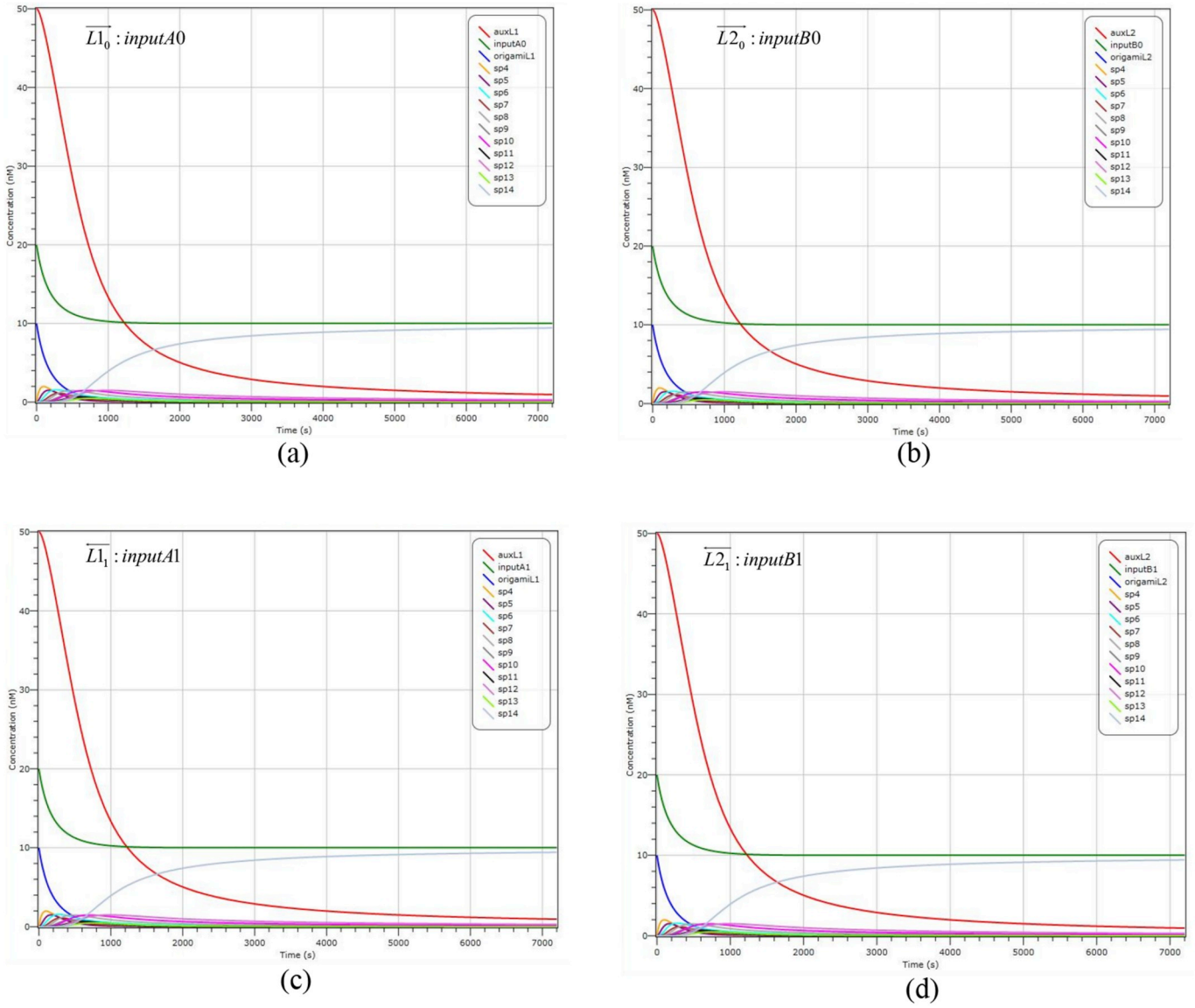

Fig. 8. The simulation diagram by Visual DSD.

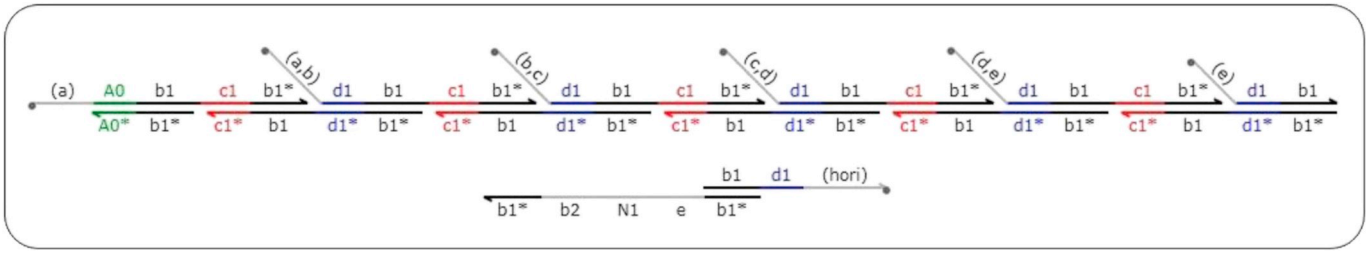

Fig. 9. Schematic diagram of the linkage of the final product on path. $\overrightarrow{L1_0}$

processes; moreover, DNA origami-based strategies can be used for the assembly of large programmable structures. Therefore, we envisage that the system will be used to some extent in the fields of biosensors and drug delivery, which will be the focus of our upcoming work.

Conflicts of interest

Authors have no conflicts of interest to disclose.

Acknowledgments

The authors would like to thank every author appearing in the references. This work was supported by National Natural Science Foundation of China [NO. 61672001, NO. 61702008] and National Natural Science Foundation of Anhui [NO.1808085MF193]. First author would like to acknowledge other authors for their valuable comments on this paper.

References

[1] L.M. Adleman, Molecular computation of solutions to combinatorial problems, Science 266 (5187) (1994) 1021–1024.
[2] R.M. Dirks, N.A. Pierce, Triggered amplification by hybridization chain reaction, Proc. Natl. Acad. Sci. Unit. States Am. 101 (43) (2004) 15275–15278.
[3] D. Yang, Y. Tang, P. Miao, Hybridization chain reaction directed DNA superstructures assembly for biosensing applications, Trends Anal. Chem. 94 (2017) 1–13.
[4] Q. Xiao, J. Wu, P. Dang, et al., Multiplexed chemiluminescence imaging assay of protein biomarkers using DNA microarray with proximity binding-induced hybridization chain reaction amplification, Anal. Chim. Acta 1032 (2018) 130–137.
[5] Z. Li, L. Tingting, S. Ruidi, et al., A label-free light-up fluorescent sensing platform based upon hybridization chain reaction amplification and DNA triplex assembly, Talanta 189 (2018) 137–142.
[6] P.W. Rothemund, Folding DNA to create nanoscale shapes and patterns, Nature 440 (7082) (2006) 297–302.
[7] L.L. Qian, Y. Wang, Z. Zhang, et al., Analogic China map constructed by DNA, Chin. Sci. Bull. 51 (24) (2006) 2973–2976.
[8] Y. Ke, J. Sharma, M. Liu, K. Jahn, Y. Liu, H. Yan, Scaffolded DNA origami of a DNA tetrahedron molecular container, Nano Lett. 9 (2009) 2445–2447.
[9] M. Pilo-Pais, S. Goldberg, E. Samano, T.H. LaBean, G. Finkelstein, Connecting the nanodots: programmable nano-fabrication of fused metal shapes on DNA templates, Nano Lett. 11 (8) (2011) 3489–3492.
[10] H. Gu, J. Chao, S.J. Xiao, et al., A proximity-based programmable DNA nanoscale assembly line, Nature 465 (2010) 202–205.
[11] H. Pei, L. Liang, G. Yao, et al., Inside back cover: reconfigurable three-dimensional DNA nanostructures for the construction of intracellular logic sensors, Angew. Chem. Int. Ed. 51 (36) (2012) 9020–9024.
[12] T.E. Tomov, R. Tsukanov, M. Liber, et al., Rational design of DNA motors: fuel optimization through single-molecule fluorescence, J. Am. Chem. Soc. 135 (32) (2013) 11935–11941.
[13] Y. Amir, E. Benishay, D. Levner, et al., Universal computing by DNA origami robots in a living animal, Nat. Nanotechnol. 9 (5) (2014) 353–357.
[14] D. Wang, Y. Fu, J. Yan, B. Zhao, B. Dai, J. Chao, H. Liu, D. He, Y. Zhang, C. Fan, S. Song, Molecular logic gates on DNA origami nanostructures for MicroRNA diagnostics, Anal. Chem. 86 (2014) 1932–1936.
[15] D. Koirala, P. Shrestha, T. Emura, K. Hidaka, S. Mandal, M. Endo, H. Sugiyama, H. Mao, Single-molecule mechanochemical sensing using DNA origami nanostructures, Angew. Chem. Int. Ed. 53 (2014) 8137–8141.
[16] J. Yang, Z. Song, S. Liu, et al., Dynamically arranging gold nanoparticles on DNA origami for molecular logic gates, ACS Appl. Mater. Interfaces 8 (34) (2016) 22451–22456.
[17] C. Zhang, J. Yang, S. Jiang, Y. Liu, H. Yan, DNAzyme-based logic gate-mediated DNA self-assembly, Nano Lett. 16 (1) (2016) 736–741.
[18] G. Tikhomirov, P. Petersen, L. Qian, et al., Fractal assembly of micrometre-scale DNA origami arrays with arbitrary patterns, Nature 552 (7683) (2017) 67–71.
[19] J. Chao, J. Wang, F. Wang, et al., Solving mazes with single-molecule DNA navigators, Nat. Mater. 18 (3) (2019) 273–279.
[20] M.S.L. Tang, C.C. Shiu, M. Godonoga, et al., An aptamer-enabled DNA nanobox for protein sensing, Nanomed. Nanotechnol. Biol. Med. 14 (2018) 1161–1168.
[21] H. Wang, J. Zheng, Y. Sun, T. Li, Cellular environment-responsive intelligent DNA logic circuits for controllable molecular sensing, Biosens. Bioelectron. 117 (2018) 729–735.
[22] Z. Zhang, M.M. Ali, M.A. Eckert, et al., A Polyvalent Aptamer System for Targeted Drug Delivery Biomaterials vol. 34, (2013), pp. 9728–9735 (37).
[23] X. Ouyang, J. Li, H. Liu, et al., Self-assembly of DNA-based drug delivery nanocarriers with rolling circle amplification, Methods 67 (2) (2014) 198–204.
[24] A. Rozita, M. Amir, R. Mohammad, et al., Application of hairpin DNA-based biosensors with various signal amplification strategies in clinical diagnosis, Biosens. Bioelectron. 129 (2019) 164–174.
[25] D. Wu, L. Wang, W. Li, et al., DNA nanostructure-based drug delivery nanosystems in cancer therapy, Int. J. Pharm. 533 (2017) 169–178.
[26] S.D. Mason, Y.N. Tang, Y.Y. Li, et al., Emerging bioanalytical applications of DNA walkers, Trac. Trends Anal. Chem. 107 (2018) 212–221.
[27] D. Mo, M.R. Lakin, D. Stefanovic, Logic circuits based on molecular spider systems, Biosystems 146 (2016) 10–25.
[28] T.G.W. Edwardson, K.L. Lau, D. Bousmail, C.J. Serpell, H.F. Sleiman, Transfer of molecular recognition information from DNA nanostructures to gold nanoparticles, Nat. Chem. 8 (2016) 162–170.
[29] Y. Zhang, et al., Transfer of two-dimensional oligonucleotide patterns onto stereocontrolled plasmonic nanostructures through DNA-origami-based nanoimprinting lithography, Angew. Chem. Int. Ed. 55 (2016) 8036–8040.
[30] Z. Zhang, Y. Yang, F.C. Pincet, M. Llaguno, C. Lin, Placing and shaping liposomes with reconfigur ble DNA nanocages, Nat. Chem. 9 (2017) 653–659.
[31] G. Chatterjee, N. Dalchau, R.A. Muscat, A. Phillips, G. Seelig, A spatially localized architecture for fast and modular DNA computing, Nat. Nanotechnol. 12 (2017) 920–927.
[32] K. Sergio, W.J. Paschoalino, L.T. Kubota, Supramolecular DNA origami nanostructures for use in bioanalytical applications, Trac. Trends Anal. Chem. 108 (2018) 88–97.
[33] K.E. Bujold, Aurélie Lacroix, H.F. Sleiman, DNA nanostructures at the interface with biology, Chemie 4 (2018) 495–521.
[34] T. Fu, Y. Lyu, H. Liu, et al., DNA-based dynamic reaction networks, Trends Biochem. Sci. 43 (7) (2018) 457–560.